Partitioning of a Scaled Shallow-Buried Near-Field Blast Load

J.D. Reinecke[1] , F.J. Beetge[2], I. Horsfall[3], M. Miaymbo[1]

[1]*Council for Scientific and Industrial Research (CSIR), Meiring Naude Drive, Pretoria , South Africa*
[2]*Armaments Corporation of South Africa Limited (Armscor), 370 Nossob Street, Erasmuskloof Ext 4, Pretoria, South Africa*
[2]*Cranfield University, Defence and Security, Shrivenham, United Kingdom*
Corresponding Author: dreinecke@csir.co.za

INTRODUCTION

Buried blast threats have been used for many years in both conventional and unconventional warfare. They are cheap, easily hidden, remain viable for extremely long periods after deployment and are effective, focusing the resulting blast products and ejecta vertically upward towards the target when finally initiated. Although extremely effective measures have been developed and deployed to protect vehicles against buried blast threats (Camp, Heitman 2014, Stiff 1986) ongoing research is required and is indeed continuing to develop and enable more effective and efficient passive and active landmine and IED protection systems for the mounted and dismounted soldier.

Characterization of threats is the first step towards any protection research efforts. For buried blast load the characterization is complicated due to the interrelationship of burial media characteristics, charge type and shape, depth of burial (DOB), presence of , shape and distance to a near-field target (stand-off distance - SOD). Various researchers (Cooper 1996, Fourney, Leiste et al. 2005, Cullis 2001, Braid 2002, Smith, Hetherington 1994, Snyman 2010) have defined a number of temporal phases that occur when a shallow buried near-field blast is detonated. Although some authors expand these phenomena, or constituents, while others combine them, they can in general, be presented in order of temporal occurrence at the target as: shock, soil cap and blast front, blast wind (detonation products), soil ejecta including casing fragments and secondary burn effects.

To date impulse has been primarily used to quantify a blast load in terms of the various dependent variables noted above. Although impulse is a robust parameter that scales well and has a large research and empirical data set to equate it to target damage, impulse lumps all the temporal phenomena developed by a buried blast load into a single value (Braid 2002, Held 2004, Karagiozova, Langdon et al. 2010, Smith, Hetherington 1994, Clarke, Fay et al. 2014) . Dynamic side-on pressure measurements can and have been used in conjunction with impulse to characterize blast and as a result give insight into the temporal phasing of a blast load. However, these measurements do not quantify density and stagnation effects of a blast load. Most impulse measurement test rigs employ known heavy inertial masses that are either vertically or horizontally orientated and then utilize either or both initial velocity and maximum displacement to calculate the impulse transmitted to the target by the blast (Zakrisson, Wikman et al. 2008, Denis M. Bergeron, Hlady et al. 2002, Held 2004, Grujicic, Pandurangan et al. 2007, Pickering, Chung Kim Yuen et al. 2012, Karagiozova, Nurick et al. 2009). A small number blast test rigs have been developed that measure the force-time response of a target to quantify free-in air or buried blast load (Snyman, Reinecke 2006, McDonald 2013, McDonald 2013) however, not all of this work has been published.

Based on literature various authors have proposed a contribution allocation of the various defined phases to the total blast load seen by a target, however these appear to have been based on free-in-air or buried blast without near-field targets, computational modelling or subjective assessment rather than specific quantification. This paper presents the quantification method and discusses the initial outcomes of a research effort to quantify the

blast contribution of a shallow buried near-field blast load in terms of the phased force-time response of the target or simply put, to partition a shallow buried near field blast load.

EXPERIMENTAL SETUP AND PROCEDURE
The research was divided into two steps, firstly to quantify the ejecta formation in terms of side-on blast pressure-time, blast velocity and mass of soil ejected and secondly to quantify the force-time response of a near-field target subjected to a specific scaled near-field shallow buried blast load.

Test Rig: Due to the aggressive nature of full-scale shallow buried blast loads and the cost and time advantages of scaled threats this research focused on a Hopkinson and Geometrically Similar scaled charges and targets. A suitably scaled test rig utilizing four piezoelectric load cells was developed for this research (Reinecke, Horsfall et al. 2014). The scaled test rig consists of two assemblies namely a soil bin and a removable target assembly. The removable target assembly comprises a rigid 360 mm diameter 10 mm thick circular target plate that is bolted to a machined short circular steel tube. The target plate / tube assembly is attached to a mounting plate (spider) sandwiching four load cells between the tube wall and the spider. The spider is 'rigidly' attached to the soil bin through four V-shaped arms using machined cross bolts. To measure target global displacement an instrumentation frame is placed over the test rig and LVDT's mounted against the back of the spider. The test rig assembly is shown in Figure 1.
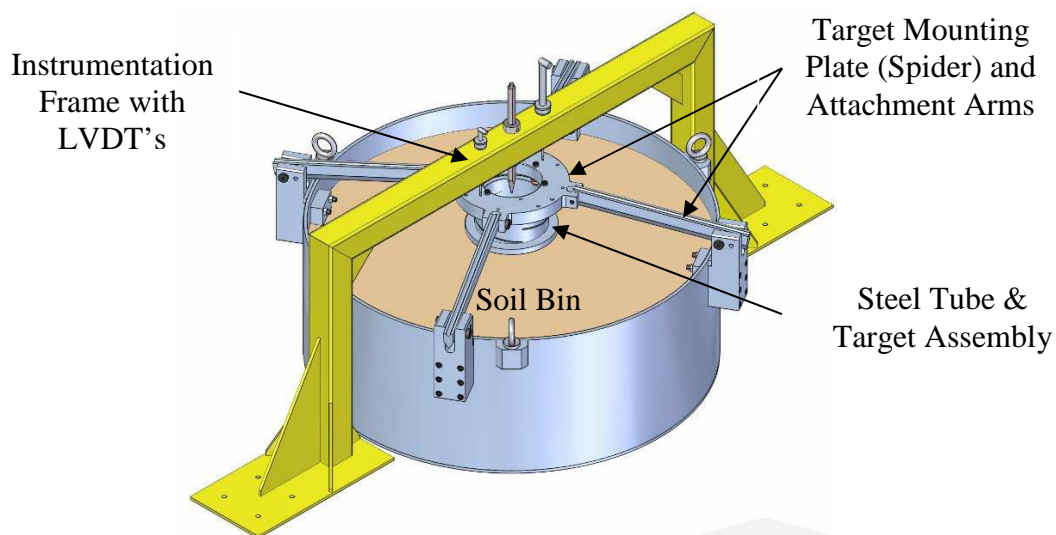
Figure 1 Scaled Test Rig Assembly

Prior to testing the target assembly is torqued against the spider to approximately 50% of the nominal force capacity of the load cells. This effectively creates a preloaded spring damper force measurement system whereby the total load applied to the target is transmitted through the four load cells. The target plate can have a variety of sensors such as side on and face on pressure sensors and force sensors fitted to further quantitatively explore the target face loads. To quantify shallow buried soil ejecta in terms side-on pressure and actual mass of soil ejected the measurement head assembly is removed. A smaller diameter bin is filled with test soil, weighed and then inserted into the partially filled main soil bin. The area around the inserted bin is then back filled with the same test soil. A single side-on pressure probe was then placed over the center of the charge once it was inserted and covered with soil. This set up is shown in Figure 2.

Test Measurements: The primary measurement with the near-field test rig was the force-time response of the target assembly. For the soil ejecta tests high speed imaging, side on pressure

and mass of soil ejecta were measured. For both experiments the primary and secondary crater diameters and depths were measured.

Figure 2: Soil ejecta test set-up

Test Method: The soil used for these tests was standard commercial river sand. Prior to these tests the bulk density and moisture content was measured and recorded using a Troxler surface gauge. The soil was not compacted. For the soil ejecta tests the inner bin was carefully removed after each test and weighed. The difference between the initial and after test masses was deemed to be the mass of soil ejected. After each test, contaminated soil was removed from the test bin and any remaining soil was mixed with fresh soil from the soil stock until the inner bin was full

The flat cylindrical PE4 test charges were hand formed into machined PVC cups. A forming tool was used to create a detonator cavity that ensured the detonator seating depth was kept constant for each test. For these specific tests the DOB was set as close as possible to 7.2 mm with a target SOD of 72 mm. A special leveling tool was developed to facilitate this process. These parameters give a scaled distance (z) of 0.29 which fits within published near-field parameters as defined by (Smith, Hetherington 1994).

At least two tests were executed per test point for the near-field tests and at least four tests per test point for the soil ejecta quantification tests. For all tests the initiation of the detonator was used as a common trigger signal for data recording. As no published commonly accepted definition of shallow buried blast threats was found in the reviewed literature, additional secondary data from similar buried blast trials but with a larger test charge, scaled DOB and SOD executed at Cranfield University as part of a master's program (McDonald 2013) was processed and compared to the obtained near-field test results. Lastly the force-time results were compared to larger scaled TNT tests executed on a different CSIR test rig.

Data Processing: The force-time test data was summed and zeroed to provide the net total target force-time response for each test. This data was then inspected and temporally partitioned according to occurrence of force peaks. The force time data was then high-pass filtered prior to integrating to calculate both the total impulse as well as the percentage impulse contribution of each phase, as defined by the temporal partitioning. For the soil ejecta the high-speed video of blast development and ejecta formation process was inspected and analyzed. A particular effort was made to identify initial detonation shock waves transmitted to the air from the soil surface as well as the subsequent morphology of the blast. The velocity of the blast front and any observed shock waves was determined from the distance-time plots as obtained within Image Systems TEMA® software. The crater volumes were calculated based on the measured test data and compared to the measured ejecta mass.

RESULTS
Soil Ejecta: As initially reported by (Freitas, Bigger et al. 2014) the two distinct ejecta phases were observed. Figure 3 shows the initial high velocity ejecta phase as it is ending and

transitioning to the low speed soil ejecta phase and the end of the second low speed soil ejecta phase. The measured ejecta base (stem) diameters that were measured and reported are indicated here.
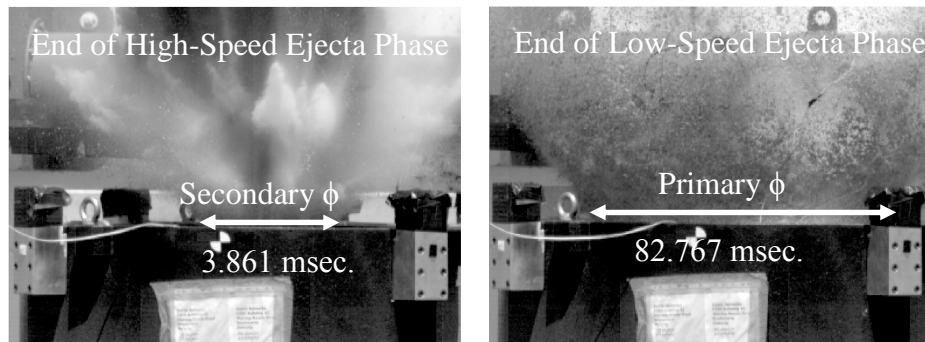
Figure 3: Shallow buried ejecta morphology

Table 1 summarizes both the averaged maximum blast front velocity and the blast front velocity at the SOD of 72 mm showing the deceleration of the blast front.

Table 1: Blast front velocities

	Shallow Buried	
	Averaged m/s	Std. Dev m/s
Maximum Velocity	1640	274
Velocity @ 72 mm	1438	153

Figure 4 presents two captured shallow buried side-on pressure-time traces. The variability inherent with buried blast and much reported is evident in the different blast morphologies shown.
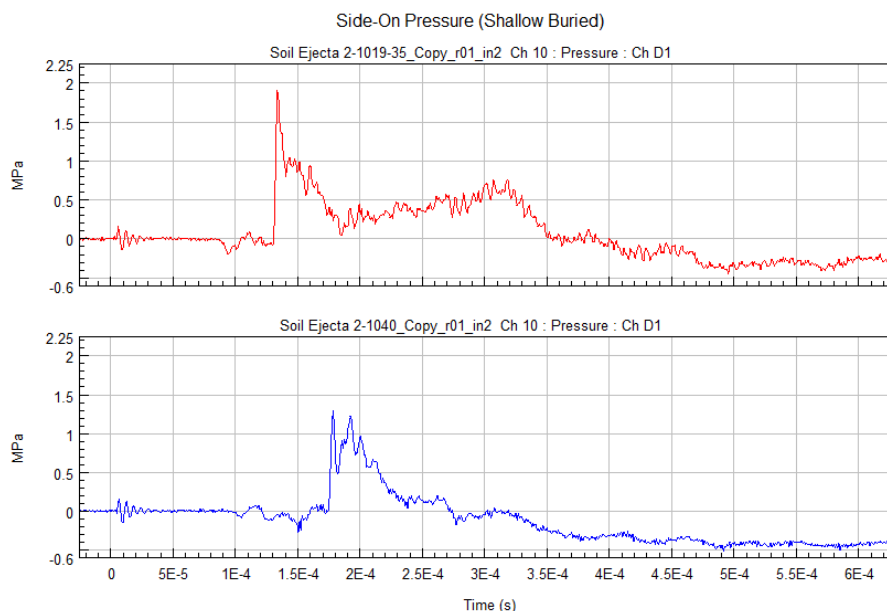
Figure 4: Side-on pressure for shallow buried blast (SOD 200 mm)

Table 2 presents the average crater dimensions obtained with both the ejecta tests and the near-field target tests. The standard deviation for each parameter is noted in the second row. The estimated ejecta mass is based on a dual cone volume approximation using the measured primary and secondary crater dimensions (*RSA-MIL-STD-37 Issue 3 Landmine Protected Wheeled Vehicles: Design, Development and Evaluation of. February 2005*) .

Table 2: Crater dimensions, estimated and measured ejecta mass

Primary Crater Ø mm	Primary Crater Depth mm	Secondary Crater Ø mm	Secondary Crater Depth mm	Estimated Ejecta Mass kg	Measured Ejecta Mass kg
Ejecta Tests					
646	158	350	54	24.8	13.0
5	13	18	10	1.8	1.7
Near-Field Target Tests					
755	151	245	100	-	-
5	17	55	21	-	-

Force-Time: Figure 5 shows the target force-time response to a scaled near-field shallow buried blast load. The complete response signal is shown to the left and the initial positive force-time only response is presented on the right. Only the first positive force phase is of interest here and the response after this initial loading is considered the damped elastic unloading of the test rig and target assembly. Three force peaks are seen within this initial positive signal, for this work the first peak is considered the first loading phase with the latter two peaks being defined as the second loading phase.
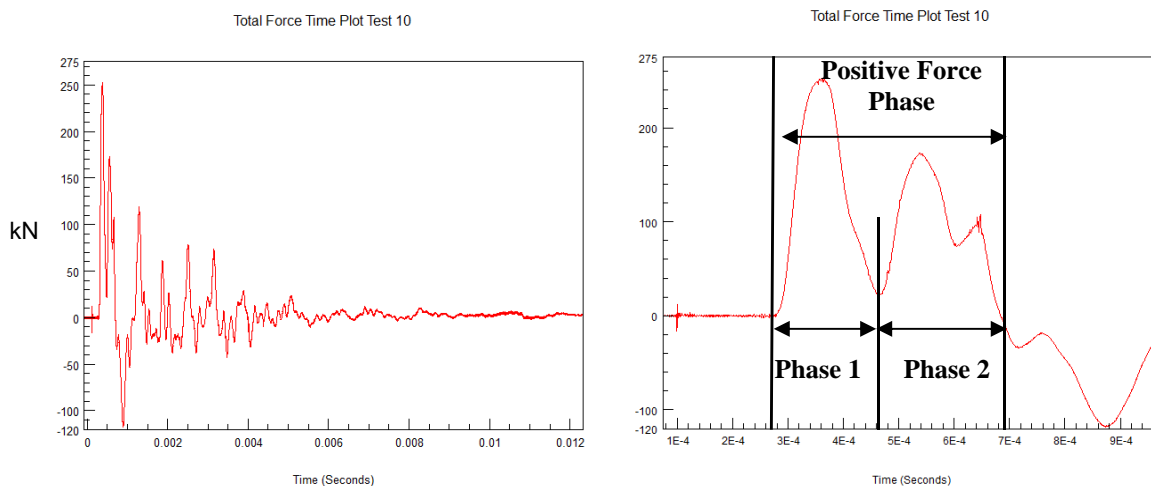
Figure 5: Near-field target force-time response with complete response signal is shown to the left and the initial positive force-time only response is presented on the right

DISCUSSION

Soil Ejecta: The morphology of the side-on pressure displays a variable phased pressure that is developed with buried blast that decays slower than a classic free in air blast pressure pulse and has a reflected pressure occurrence at a later time. This is attributed to the initial blast front followed by the containment and focusing effects of the soil (Snyman 2009, Deshpande, McMeeking et al.). The variability in peak side-on pressure measurement is attributed to the variable and ragged blast front that forms during shallow buried blast because of the soil cap. The side-on pressure data signal anomalies present prior to the arrival of the blast front are attributed to breakout of ionized detonation products interacting the sensor and no precautions were taken to minimize these effects.

The ejecta tests show that as reported by (Freitas, Bigger et al. 2014) which references work by Bangash and (Deshpande, McMeeking et al.) there are at least two distinct soil ejecta phases with shallow buried blast, an initial high speed ejecta phase that lasts between 2-4 milliseconds and a second low speed soil ejecta phase that then continues for 80-100 milliseconds. The base diameter of the slow speed ejecta phase cloud continues to grow

laterally as an expanding hollow tube at about 4 m/s with vertical ejecta velocities of between 10 and 30 m/s for ejected larger soil clumps. The side-on pressure results without a near-field target present show that the positive pressure loading is over with the negative phase starting within 250 µs after blast front arrival. The slow speed ejecta phase is characterized by a dominate heave with low soil velocity moving the soil over a short distance laterally and with a large amount of soil being deposited next to the crater rim. The majority of the ejected soil is expelled in this phase and is thought to contribute minimally to the total target loading; this position is supported by the recorded pressure and force time response of the target. The blast pressure loads the soil over a short period of a few hundred microseconds (Eridon, James. Zelenik,Tom. Bogalev, Alex. 2014) but due to its large inertial mass the surrounding the soil starts moving, primarily laterally but with some vertical component, starting only after milliseconds after detonation, which is long after the blast gases have been vented upwards.

The diameter of the high speed ejecta phase stem corresponds to the secondary crater diameter while the primary crater corresponds with the base diameter of the ejecta stem at the end of the slow ejecta speed phase. The primary crater dimensions when a near-field target is present are slightly larger and the secondary crater is slightly smaller than without the target. This near-field target reflected pressure is expected to increase the duration of the positive pressure phase but not sufficiently to result in the tenfold increase. This longer duration reflected pressure exacerbates the outward expansion of the slow speed ejecta phase resulting in a larger primary crater while compressing the already formed secondary crater resulting in a reduction of this diameter while increasing the secondary crater depth. As the estimated ejecta mass (ca. 24 kg) is nearly double that of the measured ejecta mass (ca. 13 kg) crater dimensions are not a good indicator of ejecta mass.

Force-Time: The initial positive force-time target response indicates that there is indeed a phased target reaction as a result the phased blast load. Initial inspection reveals that for near-field loading there are at least three phases, with a large initial load that decreases rapidly only to increase again and then decay more gradually followed by a third another much smaller and more gradual increase before the force become negative as the target unloads downwards. This is expected with the blast front impact forming the initial rapid force peak which starts to unload while the following blast wind starts to build up reflected pressure creating the second loading phase. The source of the third peak is not immediately evident, for larger charges it would be expected to represent the contribution of secondary burn effects however this was not expected for the smaller test charges. Based on secondary test data (McDonald 2013) this additional phase becomes apparent as the target is brought closer to the soil and is thus possibly due to additional reflection or secondary burn effects. The first loading phase contributed on average 52% of the total positive phase impulse for a scaled blast load. This is much higher contribution than what has been observed with larger scale tests (around 20%) indicating that there are blast loading aspects of near-field shallow buried blast that do not scale (Mostert July 2015).

No clear separate shock wave could be identified for any of the shallow buried tests nor was any separate precursor shock seen on the side-on pressure data within the near-field SOD of interest (72 mm). High speed video analysis only shows a bow wave shock forming at the blast front. This shock was seen to detach and progress outwards only after impact with the target would have occurred. Secondary deep buried blast test data (McDonald 2013) video analysis revealed the formation of a air shock (± 400 m/s) that was seen to be transmitted by the detonation shock reflection at the soil surface. Being deep buried the blast fronts were only moving at an average of 230 m/s, thus the weak shock moved away from the blast ejecta front and impacted the target first, reflecting back into the approaching blast front and not contributing materially to the transferred blast load. For shallow buried blast loads, as there was no precursor shock impacting the target prior to the blast front, taking the mass of the soil

cap above the test charge and multiplying this by the blast front velocity resulted in a approximated impact impulse value that is very close to that derived from the measured target phase one force response. This first phase correlation did not extend to secondary data analyzed for deep buried blast where the initial force phase impulse contribution is higher than the simple momentum of the soil cap indicating that a more complex loading is present and the initial force phase impulse contribution is more. This implies that the target force response morphology is affected by the DOB and SOD.

CONCLUSIONS

A research method to partition and quantify a shallow buried blast and the associated results using a combination of scaled soil ejecta and near-field target shallow buried blast tests were presented. The results indicate there is a temporally phased blast loading and target force response to a shallow and deep buried blast loads and the initial loading phase contribution to the blast load were quantified. There is no separate precursor air shock for shallow buried blast load and the initial loading phase impulse appears to be primarily from the soil cap impact momentum transfer. For scaled tests the first impact load contributes about half the total target impulse load. The subsequent force-time target response indicates that there is an additional third phase response during the reflected pressure loading phase. The source of this loading is thought to be either additional near field target response or possibly secondary burn and requires additional investigation to determine. Other than the soil cap, soil ejecta contributes very little to the total blast load as the main mass of ejecta is expelled much later than both the initial blast pressure loading and the resultant force-time load response of the target. Lastly crater volume is not a good predictor of ejecta mass.

REFERENCES

RSA-MIL-STD-37 Issue 3 Landmine Protected Wheeled Vehicles: Design, Development and Evaluation of. February 2005.

BRAID, M.P., 2002. *Experimental investigation and analysis of the effects of anti-personnel landmine blasts.*

CAMP, S. and HEITMAN, H.M., 2014. *Surviving the Ride: A Pictorial History of South African-Manufactured Mine Protected Vehicles.* 1 edn. 30 Degrees South.

CLARKE, S.D., FAY, S.D., TYAS, A., J. WARREN, J., RIGBY, S., ELGY, I. and LIVESEY, R., 2014. REPEATABILITY OF BURIED CHARGE TESTING. *Military Application of Blast and Shock, .*

COOPER, P.W., 1996. *Explosives engineering.* Vch Pub.

CULLIS, I.G., 2001. Blast waves and how they interact with structures. *Journal of the Royal Army Medical Corps,* **147**(1), pp. 16-26.

DENIS M. BERGERON, D.M., HLADY, S.L. and BRAID, M.P., 2002. Pendulum Technique to Measure Land Mine Blast Loading.

DESHPANDE, V.S., MCMEEKING, R.M., WADLEY, H.N.G. and EVANS, A.G., Constitutive Model for Predicting dynamic interactions between soil ejecta and structural panels.

ERIDON, JAMES. ZELENIK,TOM. BOGALEV, ALEX., 2014. Blast Distribution from Buried Charges, 2014.

FOURNEY, W.L., LEISTE, U., BONENBERGER, R. and GOODINGS, D.J., 2005. Mechanism of loading on plates due to explosive detonation. *Fragblast,* **9**(4), pp. 205-217.

FREITAS, C.J., BIGGER, R.P., THOMAS, J.P. and MACKIEWICZ, J.F., 2014. Threat Characterization Methodology for IED Post-Detonation Environments to Dismounted Warfighters, *PASS2014 Proceedings*, 8-12 September 2014, Cambridge UK 2014.

GRUJICIC, M., PANDURANGAN, B., HUANG, Y., CHEESEMAN, B., ROY, W. and SKAGGS, R., 2007. *Impulse loading resulting from shallow buried explosives in water-saturated sand.* SAGE Publications.

HELD, M., 2004. Blast Effects with the Held Momentum Method, *21st, International symposium on ballistics* 2004.

KARAGIOZOVA, D., LANGDON, G.S., NURICK, G.N. and CHUNG KIM YUEN, S., 2010. Simulation of the response of fibre–metal laminates to localised blast loading. *International Journal of Impact Engineering,* **37**(6), pp. 766-782.

KARAGIOZOVA, D., NURICK, G.N., LANGDON, G.S., YUEN, S.C.K., CHI, Y. and BARTLE, S., 2009. Response of flexible sandwich-type panels to blast loading. *Composites Science and Technology,* **69**(6), pp. 754-763.

MCDONALD, A.B., 2013. *The Response and applied Pressure of Quadrangular Plates to Buried Charges.* Cranfiled University (Defence): .

MOSTERT, F.J., July 2015. *Discussion on initial results.*

PICKERING, E.G., CHUNG KIM YUEN, S., NURICK, G.N. and HAW, P., 2012. The response of quadrangular plates to buried charges. *International Journal of Impact Engineering,* **49**(0), pp. 103-114.

REINECKE, J.D., HORSFALL, L. and SNYMAN, I., 2014. Development of a Scaled Shallow-Buried Near-Field Blast Load Test Rig. *85 TH SHOCK AND VIBRATION SYMPOSIUM 26 – 29 OCTOBER,* .

SMITH, P.D. and HETHERINGTON, J.G., 1994. *Blast and ballistic loading of structures.* CRC Press.

SNYMAN, I.M., 2009. *Blast Loading Quantification : Research Strategy, Literature Review and Experimental Design.* GLBL-AG900-09-003 Rev 1. CSIR.

SNYMAN, I.M. and REINECKE, J.D., 2006. MEASURING THE IMPULSE FROM AN EXPLOSIVE CHARGE. *Conference: Ballistics Symposium South Africa, At Denel-OTB, Bredasdorp,* .

SNYMAN, I.M., 2010. Impulsive loading events and similarity scaling. *Engineering Structures,* **32**(3), pp. 886-896.

STIFF, P., 1986. *Taming the landmine.* Galago.

ZAKRISSON, B., WIKMAN, B. and JOHANSSON, B., 2008. Half scale experiments with rig for measuring structural deformation and impulse transfer from land mines, *Proceedings of the 24th International Symposium on Ballistics,(September 22–26, New Orleans USA), DEStech Publications Inc* 2008, pp. 497-504.